

Single Chain Polymeric Nanoparticles as Selective Hydrophobic Reaction Spaces in Water

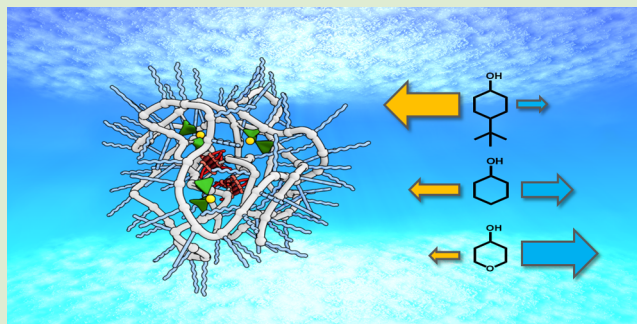
Müge Artar,[†] Erik R. J. Souren,[†] Takaya Terashima,[‡] E. W. Meijer,^{*,†} and Anja R. A. Palmans^{*,†}

[†]Laboratory of Macromolecular and Organic Chemistry and Institute for Complex Molecular Systems, Eindhoven University of Technology, P.O. Box 513, 5600 MB Eindhoven, The Netherlands

[‡]Department of Polymer Chemistry, Graduate School of Engineering, Kyoto University, Katsura, Nishikyo-ku, Kyoto 615-8510, Japan

S Supporting Information

ABSTRACT: A Ru(II)-based catalyst trapped within an amphiphilic, folded polymer is employed for the oxidation of secondary alcohols to their corresponding ketones using *t*BuOOH as the oxidant. Under the applied catalytic conditions, the polymer catalyst forms a compartmentalized structure with a hydrophobic interior. We selected secondary alcohols that differ in hydrophobicity, reactivity, and steric hindrance as substrates, with the aim to elucidate how this affects the rate and the end conversion of the oxidation reaction. Our investigations show that the Ru(II)-based catalyst is very efficient for oxidation reactions in water. Moreover, high selectivity toward the more hydrophobic substrate is observed, which originates from the hydrophobic interior of the compartmentalized catalyst system. This hydrophobic selectivity is also observed in the reverse reaction, the transfer hydrogenation.



The design of systems that perform catalysis in a highly selective manner has attracted considerable attention, not only out of academic interest, but also because of their potential in industrial applications.^{1–4} Enzymes achieve selective and efficient catalysis via a combination of hydrophilic/hydrophobic domains, size, shape, and charge recognition mechanisms at the active sites.^{5–7} In search for synthetic approaches to achieve enzyme-like selectivity and activity in catalytic conversions, hydrophobic effects such as in cross-linked nanoparticles,⁸ micellar structures,^{9–11} hydrogels,^{12–14} star polymers,¹⁵ and polymersomes,¹⁶ as well as hydrophobic reagents¹⁷ and size effects,¹⁸ have been explored. In addition to these, single chain technology,¹⁹ the transformation of an individual polymer chain into a folded/collapsed nanoparticle, has been evaluated to create active and selective catalysts in organic media²⁰ and in water.²¹ The advantage of this approach is the easy access to compartmentalized, well-defined, unimolecular nanoreactors of nanometer-size, affording homogeneous catalysis solutions. Notably, the supramolecular folding of polymer chains into single chain polymeric nanoparticles (SCPNS), in which a dynamic and adaptive reaction compartment is created, has resulted in efficient catalysis in water. In contrast to the rather dense and kinetically frozen hydrophobic compartments usually applied,^{8–16} these dynamic SCPNs possess a compact yet responsive structure and are straightforward to synthesize.^{21,22} Their activity results from the formation of a hydrophobic interior via either benzene-1,3,5-tricarboxamide (BTA) self-assembly, resulting in a chiral, structured inner compartment, and/or the diphenylphosphine styrene (SDP) complexation

with Ru(II).²¹ This results in the effective shielding of the catalyst from the aqueous environment.

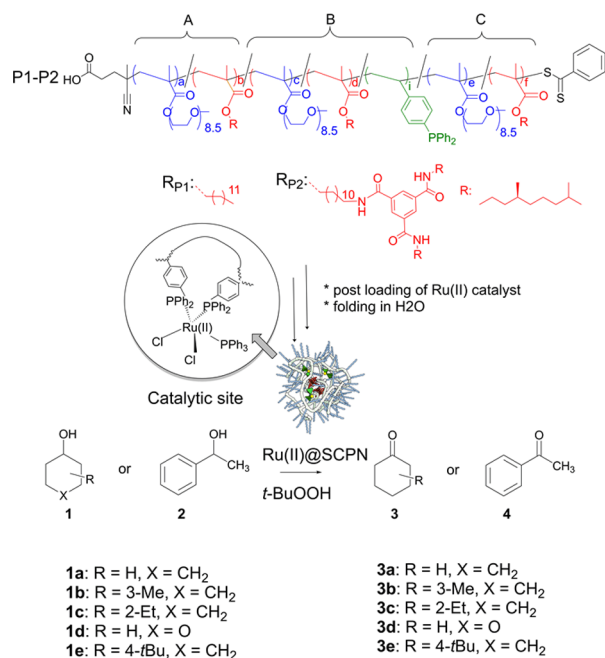
Herein, we employ amphiphilic polymers, used by us previously in the transfer hydrogenation of ketones, that fold around a Ru(II) catalyst to create a dynamic SCPN with a selective environment around an intrinsically nonselective active center.^{21a,c} It is important to achieve the folding of one single polymer chain into one SCPN, because this permits access to well-defined hydrophobic reaction spaces in which hydrophobic substrates can accumulate and catalysts that normally only function in organic media can still operate. We select lauryl-based polymer **P1** that forms a compartmentalized structure due to hydrophobic interactions²³ and BTA-based polymer **P2** that folds as a result of hydrophobic interactions in combination with directional hydrogen-bonding interactions (Scheme 1).^{21a} By applying Ru(II)@SCPNS in the presence of the oxidant *t*BuOOH, the differences in the two types of polymers could induce differences in activity and selectivity of the catalytically active SCPNs. We present here the results of the oxidation in water at RT of a set of cyclic, secondary alcohols that differ in hydrophobicity, reactivity, and steric hindrance around the alcohol function and show that a uniquely active and remarkably selective catalyst is obtained for oxidation reactions in water. In addition, we highlight the

Received: September 7, 2015

Accepted: September 9, 2015

Published: September 15, 2015



Scheme 1. Structure of Catalytically Active SCPNs for the Oxidation of Alcohols in Water and Structures of the Substrates and Products


potential of SCPNs as a general concept for compartmentalized nanoreactors for selective catalysis in water.

Methacrylate-based amphiphilic terpolymers **P1** and **P2** (Scheme 1) with a degree of polymerization (DP) of 150 were prepared by RAFT polymerization of oligo(ethylene

glycol) methyl ether methacrylate (oEGMA), ligand diphosphinostyrene (SDP), and hydrophobic lauryl methacrylate (LMA) or benzene-1,3,5-tricarboxamide-based methacrylate (BTAMA), respectively, following previously reported procedures (Table S1, Figures S1,2).^{21c} SEC traces of **P1** and **P2** (relative to PEG standards) showed unimodal peaks and molecular weights around 14 kDa, with molar mass distributions (\mathcal{D}) below 1.4 (Table S1, Figure S3). To procure a catalytically active polymer, **P1** and **P2** were loaded with RuCl₂(PPh₃)₃ (Ru(II)) using our previously reported post-encapsulation approach to create catalytic centers.^{21c} The exchange of the phosphines of Ru(II) (PPh₃)₃Cl₂ with those of the phosphines attached to the polymer backbone was monitored by ³¹P NMR (Figure S4), which revealed a quantitative immobilization of the Ru-catalyst on the polymer. **P1** and **P2** comprised around 2–3 Ru centers per polymer chain, as determined with ICP-AES. The amphiphilic polymers and their corresponding catalysts were further characterized with dynamic light scattering (DLS; Figure S5) and circular dichroism (CD) for **P2** (Figure S6). SEC measurements were not possible after Ru loading because of strong interactions of the polymers with the column. After the formation of the catalyst complex, the single chain character was preserved in both polymers, as revealed by DLS, while CD experiments showed that **P2** comprised a structured, chiral inner compartment as a result of helical BTA stacking.²¹

We first evaluated the catalytic activity of the **P1**@Ru(II) catalyst, lacking the structuring BTA units. The oxidation of cyclohexanol (**1a**) to cyclohexanone (**3a**) was performed in the presence of *t*BuOOH, a highly efficient oxidant at room temperature compared to other oxygen sources.²⁴ Samples were taken during the course of the reaction, quenched with

Table 1. Conversion, Turnover Frequency, and Log *P* Values for the Oxidation of Secondary Alcohols in Water with a SCPN System and Ru(II)-Based Catalyst^{a,j}

entry	substrate	polymer	Ru/substrate/oxidant (mM)	% conversion ^b (<i>t</i> (min))	TOF (h ⁻¹)	log <i>P</i> ^{c,f}
1	1a	P1	1/40/200	93 (13)	171	1.23 ^e
2		P2	1/40/200	93 (13)	171	
3		P1	1/40/-	0 (60)	0	
4		P1	-/40/200	0 (60)	0	
5		P1	-/40/-	0 (60)	0	
6			-/40/200	0 (60)	0	
7			1/40/200	nd ^d (60)	nd ^d	
8	2	P1	1/40/200	>99 (4)	600	1.42 ^e
9	1d	P1	1/40/200	50 (14)	86	0.06 ^f
10	1b	P2	1/40/200	>99 ^e (13)	184	1.59 ^f
11	1c	P2	1/40/200	>99 ^e (5)	480	2.33 ^f
12	1a		1/40 ^g /200	25(60)	40	1.23 ^e
	1d			25(60)	40	0.06 ^f
	1e			25(60)	40	3.06 ^{e,g,h}
13 ^k	1a	P1	1/40 ^g /200	28(60)	45	1.23 ^e
	1d			30(60)	48	0.06 ^f
	1e			28(60)	45	3.06 ^{e,g,h}
14	1a	P1	1/40 ^g /200	70 (4), 93 (12) ⁱ	186	1.23 ^e
	1d			20 (4), 54 (12) ⁱ	108	0.06 ^f
	1e			>99 (4) ⁱ	600	3.06 ^{e,g,h}

^aReactions in entries 1–5, 8–11 and 13 were performed with a polymer concentration of 18 mg mL⁻¹ at room temperature in water. ^bThe conversion was determined using GC. ^cNo enantioselectivity was observed in the oxidation (Figure S8). ^dnd = not determined, due to insolubility of RuCl₂(PPh₃)₃ in H₂O. ^eExperimentally determined log *P* values. ^fCalculated log *P* values by Molinspiration. ^gMolar ratio **1a**/**1d**/**1e** = 1:1:1. ^hThe log *P* values for the *cis* and *trans* products were averaged. ⁱFinal conversions. ^jThe reaction of entry 12 was performed in the presence of RuCl₂(PPh₃)₃ (without polymer) at RT in acetone. ^kThe reaction in entry 14 was performed with a polymer concentration of 18 mg mL⁻¹ at room temperature in acetone.

sodium metabisulfite, and analyzed with GC-MS (Figure S7). The conversion versus time plot shows a fast reaction, and after 12 min, the conversion levels off at 93% (Figure S7). The turnover frequency (TOF, mol substrate reacted per mol catalyst per hour) is 171 h^{-1} (Table 1, entry 1). The GC trace shows that no side products are formed during the oxidation reaction. In addition, the color of the catalysis mixture changed from yellow/orange to dark purple after addition of the *t*BuOOH (Figure 1a). This was due to the change in oxidation

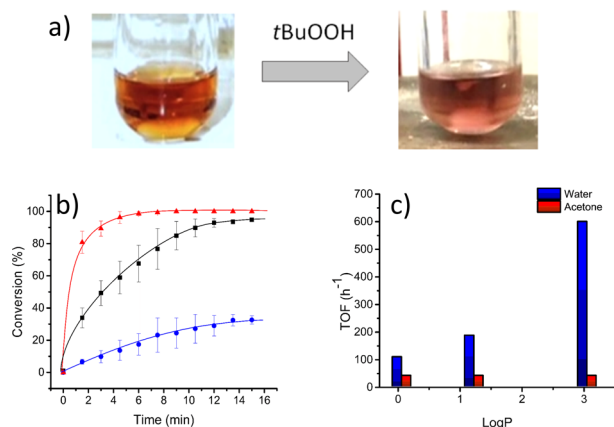


Figure 1. (a) Catalysis mixture and (b) conversion of alcohols **1a** (black squares), **1d** (blue circles), and **1e** (red triangles) as a function of time in **P1**@Ru(II)-catalyzed competitive oxidation of the three substrates in water. (c) Comparison of TOF vs log *P* in the competition experiment using **P1**@Ru(II) in water and $\text{RuCl}_2(\text{PPh}_3)_3$ in acetone. Reaction conditions: $\text{Ru}/\mathbf{1a}/\mathbf{1d}/\mathbf{1e}/t\text{BuOOH} = 0.001/0.0133/0.0133/0.0133/0.2 \text{ M}$ (17 mg/mL **P1**).

state of the ruthenium from Ru(II) to Ru(IV). Moreover, the mixture remained homogeneous and kept its purple color throughout the reaction, indicating that the catalyst remained active. Polymer **P2**, comprising a structured, chiral inner compartment, shows a similar result as **P1** (Table 1, entry 2). Control reactions were performed in which either **P1**@Ru(II) or Ru were not added to the reaction mixture. In these cases, no conversion was observed (Table 1, entries 3–7). The oxidation of 1-phenyl-ethanol (**2**), a highly reactive substrate, to acetophenone (**4**) was also evaluated using **P1**@Ru(II). The oxidation of **2** is faster compared to that of **1a**, and complete conversion was reached in 4 min (Table 1, entry 8).

The oxidations of both cyclohexanol (**1a**, Table 1, entry 1) and 1-phenylethanol proceeded very fast and to high conversions, 93 and >99%, respectively. The lack of full conversion for cyclohexanol was intriguing, and we anticipated, based on previous literature results,^{11,12} that this was related to a different log *P* value, a well-known quantity to assess the relative hydrophobicity of organic compounds. To test this, we investigated a more hydrophilic derivative, 4-tetrahydropyranol (**1d**). Interestingly, a final conversion of 54% was obtained after 15 min, corresponding to a TOF of 86 h^{-1} (Table 1, entry 9). This increase in hydrophilicity of the substrate resulted in a decrease of both the rate (TOF) and the final conversion of the substrate.²⁷ On the other hand, more hydrophobic 3-methylcyclohexanol (**1b**) and 2-ethylcyclohexanol (**1c**) were converted to >99% conversion within 15 min, corresponding to a TOF of 184 and 480 h^{-1} , respectively (Table 1, entries 10 and 11). Although **P2**@Ru(II) comprising a chiral inner compart-

ment was employed as the catalyst, no stereoselectivity was observed in the oxidations of **1b** and **1c**.

The results shown above, higher TOF and higher conversions for more hydrophobic substrates, indicate that there is a hydrophobic selectivity of the SCPN@Ru(II) system. Therefore, we performed a competition experiment in water by applying a 1:1:1 mixture of three substrates, 4-*tert*-butylcyclohexanol (**1e**), **1d**, and **1a**.²⁸ The log *P* values of these substrates differ significantly (Table 1). To assess that the chemical reactivity of the alcohols is similar, the competition experiment of the three substrates was first performed in acetone using Ru(II) (PPh_3)₃Cl₂ as the catalyst. Also, **P1**@Ru(II) was used in acetone in which the hydrophilic/hydrophobic phase separation that creates the driving force for selective accumulation of the substrates is absent. Finally, the influence of a structured inner compartment on the reaction rates was assessed by comparing **P1**@Ru(II) with **P2**@Ru(II).

In acetone, all three substrates were converted at the same rate, reaching a final conversion of 25% for Ru(II) (PPh_3)₃Cl₂ (Table 1, entry 12) and 28–30% for **P1**@Ru(II) (Table 1, entry 13). Thus, the chemical reactivity of the three substrates is identical, and selectivity is absent in the absence of a hydrophobic effect. The low end conversion is due to the applied conditions that are identical to the catalysis in water in the presence of SCPN@Ru(II). Previously, a higher end conversion (82%) was reported for the oxidation of cyclohexanol, but for higher catalyst and oxidant concentrations.²⁴ In contrast, in water using **P1**@Ru(II), the final conversion of the three substrates differs significantly (Table 1, entry 14). Furthermore, **1e** showed the fastest reaction rate, while **1d** showed the slowest reaction rate (Figure 1b). In addition, the conversion profiles for the three substrates were very similar for both catalysts **P1**@Ru(II) and **P2**@Ru(II) (Table S2, entry 1). It is important to note that the oxidations of mixtures **1a/1d** (93/50%; Table S2, entry 2) and **1a/1e** (60/>99%; Table S2, entry 3) showed similar rates and almost identical end conversions compared with the oxidation of the **1a/1d/1e** mixture. This implies that substrates are converted simultaneously rather than sequentially. In addition, the catalyst remained active, despite the incomplete conversions of **1a** and **1d**, as confirmed by a control reaction (Table S2, entry 4). Plotting the TOF as a function of the log *P* of the three substrates **1a**, **1d**, and **1e** reveals a remarkable correlation between their log *P* values and their reaction rate in water, which is absent in acetone (Figure 1c). This suggests that the hydrophobicity of the substrates plays a crucial role in the rate of the oxidation, and that there is selectivity of the compartmentalized catalyst for more apolar substrates.

To assess the reaction scope of the selectivity for more hydrophobic substrates of the compartmentalized catalysts, a 1:1:1 mixture of the ketones **3d**, **3a**, and **3e** was evaluated in the reverse reaction, the transfer hydrogenation (Table S3), to secondary alcohols **1a**, **1d**, and **1e**. Gratifyingly, this reaction showed an almost identical selectivity toward the more hydrophobic ketone (conversion **3d/3a/3e** = 30%/70%/>99%, Table S3). This indicates that the origin of selectivity is the presence of a hydrophobic reaction space. In addition, this demonstrates the wider applicability of the designed hydrophobic pocket for selective catalysis in aqueous environments.

Although our SCPN@Ru(II) system in water is slower than recently reported highly active, cationic, water-soluble Ru-complexes,²⁹ it is much faster and more efficient than the

original $\text{RuCl}_2(\text{PPh}_3)_3$ catalyst.³⁰ In addition, our system is highly selective for hydrophobic substrates. Figure 1b shows that both the rate of the oxidation reaction as well as the end conversion correlate well with the partitioning ratio of the substrates between the hydrophobic compartment created by the SCPN and water. Catalytic systems showing differences in reaction rate and end conversion have been reported before. Escuder and co-workers employed L-proline-based catalytically active hydrogels, which catalyze the aldol reaction of 4-nitrobenzaldehyde with ketones varying in polarity ($\log P$).¹² An increasing $\log P$ of the ketone gave higher yields and higher reaction rates, which was attributed to the hydrophobic structure of the hydrogel. Moreover, Neumann and co-workers used polyoxometalate-based hydrogels for the oxidation of 2-alkanols to 2-alkanones.¹³ A high selectivity was observed for the more hydrophobic substrates in competition reactions with less hydrophobic substrates, which was termed “lipophiloselectivity”. The highest lipophiloselectivity value (defined as $\text{TON}_{\text{high } \log P \text{ alcohol}}/\text{TON}_{\text{low } \log P \text{ alcohol}}$ in which TON is the turnover number) of 2.6 was found in the oxidation of 2-tetradecanol ($\log P = 6.11$ ³¹) with 2-pentanol ($\log P = 1.25$ ³¹), two substrates that differ significantly in hydrophobicity.

In our system, we ascribe the enhancement in the reaction rate of the more hydrophobic substrates to the concentrator effect, which gives rise to an increased local concentration of substrates around confined catalytic centers in water.^{17,32} The substrates partition between water and the hydrophobic pocket provided by the SCPNs, which results in an enhanced rate for the more hydrophobic substrates, owing to their relatively higher local concentration. The differences in end conversion between substrates varying in $\log P$ suggest that equilibrium is reached, despite the presence of an excess of oxidant and a catalyst that remains active. Although the catalysis mixture appears homogeneous, our system is thought to comprise a heterogeneous microstructure providing several distinctly different phases,³³ which hampers a quantitative determination of the different species in the different microenvironments. In addition, the dispersity of the SCPNs gives rise to the formation of the reaction spaces with different sizes and active sites in different types of local environments. These, in combination with (i) a complex composite of noncovalent interactions governing the traffic of reactants, active complexes, and products among these phases,³⁴ and (ii) the distribution/competition of the oxidant *t*BuOOH and its more hydrophilic byproduct *t*BuOH, make it very difficult to predict the end conversion of the different substrates.³⁴ Nevertheless, we observe lipophiloselectivities of up to 5 in our competition experiments.³⁵ This high value for chemically almost identical substrates is attributed to the flexible, sterically unconstrained structure of the catalysis environment created within the SCPNs. Remarkably, there were no significant differences between catalysts based on P1 and P2 in the competition reactions, although the latter has a more hydrophobic, structured inner compartment.^{21c} Also, no stereoselectivity was observed in the oxidation reactions when using P2. However, the presence of lauryl or BTA groups is required for catalytic activity of SCPN@Ru(II) (Table S4). Apparently, the strong Ru(II) complexation to the SDP units in combination with a hydrophobic collapse suffices to effectively shield the Ru center from the aqueous environment. At the same time, the distance between the catalytic centers and the helical BTA aggregates seems to be too large to affect the (stereo)selectivity of the reactions.

In conclusion, we employed amphiphilic polymers that fold into SCPNs and hereby create a hydrophobic environment around a Ru(II) catalytic center in order to carry out selective catalysis with an intrinsically nonselective active center. The hydrophobic reaction space results in a high local concentration of substrates around the catalytic sites, resulting in fast reactions. Moreover, we show for the first time that this system shows high selectivity toward hydrophobic substrates, both in oxidation as well as in reduction reactions. The SCPN structure allows efficient conversion of even the most water-soluble substrates, yet providing a significant selectivity for chemically almost identical substrates. As a result, compartmentalized amphiphilic nanoreactors based on SCPNs provide very efficient reaction spaces to achieve selectivity, based on hydrophobic effects.

■ ASSOCIATED CONTENT

Supporting Information

The Supporting Information is available free of charge on the ACS Publications website at DOI: 10.1021/acsmacrolett.5b00652.

Synthetic protocols, characterization methods, and instrumental data (PDF).

■ AUTHOR INFORMATION

Corresponding Authors

*E-mail: e.w.meijer@tue.nl

*E-mail: a.palmans@tue.nl

Notes

The authors declare no competing financial interest.

■ ACKNOWLEDGMENTS

This work was financially supported by The Netherlands Organization for Scientific Research (ECHO Grant 713.011.001), the Dutch Ministry of Education, Culture and Science (Gravity Program 024.001.035), and the European Research Council (FP7/2007–2013, ERC Grant Agreement 246829). A.P. would like to thank Prof. Dr. J. Meuldijk (TU/e) for insightful discussions. The ICMS Animation Studio (TU/e) is acknowledged for providing the art work.

■ REFERENCES

- (1) Weisz, P. B.; Haag, W. O.; Rodewald, P. G. *Science* **1979**, *206*, 57–58.
- (2) Dusselier, M.; Van Wouwe, P.; Dewaele, A.; Jacobs, P. A.; Sels, B. F. *Science* **2015**, *349*, 78–80.
- (3) Noyori, R. *Angew. Chem., Int. Ed.* **2002**, *41*, 2008–2022.
- (4) ten Brink, G. J.; Arends, I. W. C. E.; Sheldon, R. A. *Science* **2000**, *287*, 1636–1639.
- (5) Warshel, A. *Proc. Natl. Acad. Sci. U. S. A.* **1978**, *75*, 5250–5254.
- (6) Warshel, A. *Angew. Chem., Int. Ed.* **2014**, *53*, 10020–10031.
- (7) Garcia-Viloca, M.; Gao, J.; Karplus, M.; Truhlar, D. G. *Science* **2004**, *303*, 186–195.
- (8) Liu, Y.; Wang, Y.; Wang, Y.; Lu, J.; Piñón, V.; Weck, M. J. *Am. Chem. Soc.* **2011**, *133*, 14260–14263.
- (9) Hamasaka, G.; Muto, T.; Uozumi, Y. *Angew. Chem., Int. Ed.* **2011**, *50*, 4876–4878.
- (10) Ge, Z.; Xie, D.; Chen, D.; Jiang, X.; Zhang, Y.; Liu, H.; Liu, S. *Macromolecules* **2007**, *40*, 3538–3546.
- (11) Cotanda, P.; O'Reilly, R. K. *Chem. Commun.* **2012**, *48*, 10280–10282.
- (12) Berdugo, C.; Miravet, J. F.; Escuder, B. *Chem. Commun.* **2013**, *49*, 10608–10610.

- (13) Haimov, A.; Neumann, R. *J. Am. Chem. Soc.* **2006**, *128*, 15697–15700.
- (14) Moore, B. L.; Moatsou, D.; Lu, A.; O'Reilly, R. K. *Polym. Chem.* **2014**, *5*, 3487–3494.
- (15) Terashima, T.; Ouchi, M.; Ando, T.; Sawamoto, M. *J. Polym. Sci., Part A: Polym. Chem.* **2011**, *49*, 1061–1069.
- (16) van Oers, M. C. M.; Loai, K. E. A.; Rutjes, F. P. J. T.; van Hest, J. C. M. *Chem. Commun.* **2014**, *50*, 4040–4043.
- (17) Biscoe, M. R.; Breslow, R. *J. Am. Chem. Soc.* **2005**, *127*, 10812–10813.
- (18) Helms, B.; Fréchet, J. M. J. *Adv. Synth. Catal.* **2006**, *348*, 1125–1148.
- (19) (a) Altintas, O.; Barner-Kowollik, C. *Macromol. Rapid Commun.* **2012**, *33*, 958–971. (b) Lyon, C. K.; Prasher, A. A. M.; Hanlon, B. T.; Tuten, C. A.; Tooley, P. G.; Berda, E. B. *Polym. Chem.* **2015**, *6*, 181–197. (c) Gonzalez-Burgos, M.; Latorre-Sanchez, A.; Pomposo, J. A. *Chem. Soc. Rev.* **2015**, *44*, 6122–6142.
- (20) (a) Perez-Baena, I.; Barroso-Bujans, F.; Gasser, U.; Arbe, A.; Moreno, A. J.; Colmenero, J.; Pomposo, J. A. *ACS Macro Lett.* **2013**, *2*, 775–779. (b) Mavila, S.; Rozenberg, I.; Lemcoff, N. G. *Chem. Sci.* **2014**, *5*, 4196–4203. (c) Sanchez-Sanchez, A.; Arbe, A.; Colmenero, J.; Pomposo, J. A. *ACS Macro Lett.* **2014**, *3*, 439–443. (d) Willenbacher, J.; Altintas, O.; Trouillet, V.; Knöfel, N.; Monteiro, M. J.; Roesky, P. W.; Barner-Kowollik, C. *Polym. Chem.* **2015**, *6*, 4358–4365.
- (21) (a) Terashima, T.; Mes, T.; De Greef, T. F. A.; Gillissen, M. A. J.; Besenius, P.; Palmans, A. R. A.; Meijer, E. W. *J. Am. Chem. Soc.* **2011**, *133*, 4742–4745. (b) Huerta, E.; Stals, P. J. M.; Meijer, E. W.; Palmans, A. R. A. *Angew. Chem., Int. Ed.* **2013**, *52*, 2906–2910. (c) Artar, M.; Terashima, T.; Sawamoto, M.; Meijer, E. W.; Palmans, A. R. A. *J. Polym. Sci., Part A: Polym. Chem.* **2014**, *52*, 12–20.
- (22) (a) Gillissen, M. A. J.; Terashima, T.; Meijer, E. W.; Palmans, A. R. A.; Voets, I. K. *Macromolecules* **2013**, *46*, 4120–412. (b) Stals, P. J. M.; Gillissen, M. A. J.; Paffen, T. F. E.; de Greef, T. F. A.; Lindner, P.; Meijer, E. W.; Palmans, A. R. A.; Voets, I. K. *Macromolecules* **2014**, *47*, 2947–2954. (c) Artar, M.; Huerta, E.; Meijer, E. W.; Palmans, A. R. A. In *Sequence-Controlled Polymers: Synthesis, Self-Assembly, and Properties*; Lutz, J.-F., Meyer, T. Y., Ouchi, M., Sawamoto, M., Eds.; ACS Symposium Series 1170; American Chemical Society: Washington, DC, 2014; ch. 21, pp 313–325.
- (23) Terashima, T.; Sugita, T.; Fukae, K.; Sawamoto, M. *Macromolecules* **2014**, *47*, 589–600.
- (24) Tsuji, Y.; Ohta, T.; Ido, T.; Minbu, H.; Watanabe, Y. *J. Organomet. Chem.* **1984**, *270*, 333–341.
- (25) Sangster, J. *J. Phys. Chem. Ref. Data* **1989**, *18*, 1111–1227.
- (26) <http://www.molinspiration.com>.
- (27) To ensure activity of the catalytic system, which is prone to be deactivated by atmospheric O₂, and to test if any substrate and/or product inhibition is present in the case of **1d** oxidation, **1a** (40 mM) was added to a typical catalysis mixture of **1d** (SCPN@Ru/substate/oxidant: 1/40/200 mM) as it reached the maximum conversion around 40% in 18 min and **1a** was oxidized with 40% conversion (Table S1, entry 3). This shows that the system is active, not inhibited, and the low end conversion is due to poor partition of the water soluble **1d** in the hydrophobic reaction space.
- (28) Alcohol **1e** is water-insoluble but, in the presence of the more hydrophilic substrates, becomes soluble in the water environment.
- (29) Aliende, C.; Pérez-Manrique, M. F.; Jaloñ, A.; Manzano, B. R.; Rodríguez, A. M.; Espino, G. *Organometallics* **2012**, *31*, 6106–6123.
- (30) Murahashi, S. I.; Naota, T. *Synthesis* **1993**, 1993, 433–440.
- (31) Yalkowsky, S. H.; Valvani, S. C. *J. Pharm. Sci.* **1980**, *69*, 912–922.
- (32) Helms, B. C.; Liang, O.; Hawker, C. J.; Fréchet, J. M. J. *Macromolecules* **2005**, *38*, 5411–5415.
- (33) Chen, B.-T.; Bukhryakov, K. V.; Sougrat, R.; Rodionov, V. O. *ACS Catal.* **2015**, *5*, 1313–1317.
- (34) Engberts, J. B. F. N. *Pure Appl. Chem.* **1992**, *64*, 1653–1660.
- (35) We observed lipophiloselectivities of 1.4 (final conversion_{1e} (log P = 3.06)/final conversion_{1a} (log P = 1.23)) and 5 (final conversion_{1e} (log P = 3.06)/final conversion_{1d} (log P = -0.06)).